PERFORMANCE BOUNDS AND IDENTIFIABILITY CONDITIONS FOR LOCATION ESTIMATION IN NLOS DYNAMIC ENVIRONMENTS

Konstantinos Papakonstantinou[*]

Elliptic Laboratories AS
Oslo, Norway
Email: konstantinos@ellipticlabs.com

Dirk Slock[†]

Mobile Communications Department, Eurecom
Sophia Antipolis, France
Email: slock@eurecom.fr

ABSTRACT

The non-trivial problem of Non-Line-of-Sight localization can be attacked with the aid of geometrical channel and mobility models. This approach results in high performance algorithms but requires a combination of different sources of information, like e.g. angles, delays and Doppler shifts. In this contribution we demonstrate the high performance of such methods even in poor scattering environments. On top of that, we compare the algorithms for different scenarios and highlight the superiority of algorithms designed for channels that change dynamically due to the movement of the mobile terminal.

Index Terms— Localization, Non-Line-of-Sight, Single-Bounce, CRB, Identifiability

1. INTRODUCTION

"Traditional" geometrical localization methods, like e.g. trilateration and triangulation, can not achieve sufficient accuracy when the signal propagates in Non-Line-of-Sight (NLoS) environments. There exist two fundamentally different approaches to attack the NLoS localization problem. The first approach introduces some errors that are induced from the NLoS propagation and tries to mitigate them. The second one introduces a more accurate but also more complex representation of the environment and thus requires more sources of information, like angles, delays, Doppler shifts, i.e. more estimates of location-dependent parameters (LDP). It also introduces nuisance parameters that need to be eliminated or jointly estimated. Obviously, choosing between these two approaches, creates a performance-complexity trade-off. The second approach leads to improved accuracy at the cost of increased complexity. On the other hand, in the first approach at least some of the communications links must be LoS in order for the estimates to be accurate. Due to the non-satisfactory performance of the first approach in strictly NLoS environments, we focus on the second approach.

Choosing an appropriate -for NLoS localization- channel model, is still an open problem. Making too many assumptions on the environment leads to simplistic models, which in turn leads to powerful localization algorithms. However, their applicability is limited. On the other hand, using generic models leads to a very high-dimensional parameter estimation problem that is cumbersome to solve. Even when it can be solved, either the performance is low or the complexity incredibly high. Combining this with the previous remark, it becomes obvious that there is actually a performance-complexity-applicability trade-off. Overall, the Single-Bounce Model (SBM) [1] presented in the next section, can achieve a good trade-off, since it enables mobile terminal (MT) localization with high accuracy in numerous NLoS environments.

On top of choosing an appropriate channel model, if the MT is moving, one could integrate it with a mobility model in order to exploit the information in the time-variation of the LDP. It suffices to say that exploiting this new dimension, namely the variation in time, has great advantages in terms of performance and identifiability, which can be studied using the Fisher Information Matrix (FIM). In this work we study both in depth, complementing the work presented in [2] with new results.

Notation: For any defined vector $\boldsymbol{a}$, $\boldsymbol{A} = diag\{\boldsymbol{a}\}$ and for any defined matrix $\boldsymbol{A}$, $\boldsymbol{a} = vec\{\boldsymbol{A}\}$. Extending this, a_i will denote the ith entry of $\boldsymbol{a}$ and the $\{i,i\}$ entry of $\boldsymbol{A}$. It therefore suffices to define any of the above (a vector, a diagonal matrix or just a scalar), to define all 3.

2. CHANNEL MODEL

In order to localize a MT in a NLoS environment, the information about the the MT location contained in the multipath signal components has to be exploited. To that end, we consider only the first few arriving components and make the assumption that they have bounced only once. The use of Single

[*]The work presented in this paper has been partially funded by the Norwegian research council.

[†]Eurecom's research is partially supported by its industrial members: BMW Group Research & Technology, Bouygues Telecom, Cisco, Hitachi, ORANGE, SFR, Sharp, STMicroelectronics, Swisscom, Thales. The work presented in this paper has also been partially supported by the European FP7 projects Where2 and Newcom++.

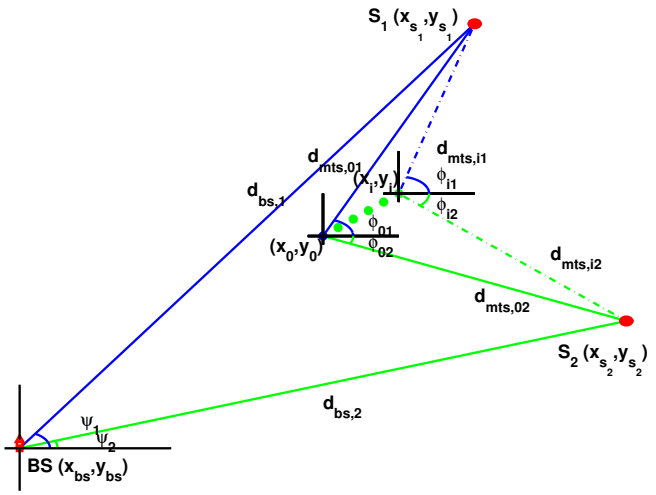

Fig. 1. Dynamic Single-Bounce Model

Bounce Model (SBM) [1] ,offers a simple one-to-one mapping between the various LDP and the coordinates of the MT and the scatterers, for static environments. For dynamic environments, a dynamic-SBM (DSBM), which is the result of the integration of a mobility model with the SBM can be used instead. This is shown in fig. 1.

Let $\boldsymbol{\phi}$, $\boldsymbol{\psi}$, $\mathbf{d}$, $\mathbf{f}_d$ denote the vectors containing the angles of arrival (AoA), angles of departure (AoD), lengths of paths and the Doppler shifts (DS) of the corresponding signal components respectively. With respect to figure 1 and using subscript ij for their entries at time instant t_i, $0 \leq i < N_t$ and corresponding to path (or scatterer) j, $1 \leq j \leq N_s$, the LDP are given by:

$$d_{ij} = d_{mts,ij} + d_{bs,ij} \tag{1}$$

$$d_{mts,ij} = \sqrt{(y_{s_j} - y_i)^2 + (x_{s_j} - x_i)^2} \tag{2}$$

$$d_{bs,ij} = d_{bs,j} = \sqrt{(y_{s_j} - y_{bs_j})^2 + (x_{s_j} - x_{bs_j})^2} \tag{3}$$

$$\psi_{ij} = \psi_j = \tfrac{\pi}{2}(1 - sgn\{x_{s_j} - x_{bs_j}\}) + \tan^{-1}\tfrac{y_{s_j} - y_{bs_j}}{x_{s_j} - x_{bs_j}} \tag{4}$$

$$\phi_{ij} = \tfrac{\pi}{2}(1 - sgn\{x_{s_j} - x_i\}) + \tan^{-1}\tfrac{y_{s_j} - y_i}{x_{s_j} - x_i} \tag{5}$$

$$f_{d,ij} = \frac{f_c}{c}\frac{\upsilon_{x_i}(x_{s_j} - x_i) + \upsilon_{y_i}(y_{s_j} - y_i)}{d_{mts,ij}} \tag{6}$$

3. FISHER INFORMATION MATRIX

Location estimation is equivalent to estimating the vector of MT coordinates, $\mathbf{p}_{mt} = [x_{mt}, y_{mt}]^t$. If the MT is moving, LDP estimates obtained at different time instances can be jointly processed for better performance. In such scenarios, there might be a need to jointly estimate $2N_m$ coefficients, where N_m is the order of the mobility model used to describe the movement of the MT. For example, for linear movement ($N_m = 1$), the speed vector $\mathbf{p}_\upsilon = [\upsilon_x, \upsilon_y]^t$, should be jointly estimated, unless its estimate already exists due to the use of e.g. inertial sensors. We refer to the above $2N_m + 2$ parameters as parameters of interest and denote the vector that contains them as $\mathbf{p}_{int}$. The rest of the unknown parameters in the problem formulation, which are the coordinates of the scatterers, are just nuisance parameters and they compose the vector $\mathbf{p}_{nui} = [\mathbf{x}_s^t, \mathbf{y}_s^t]^t$. The set of all of the above $N_\mathbf{p} = 2N_s + 2N_m + 2$ parameters compose the vector:

$$\mathbf{p} = [\mathbf{p}_{int}^t, \mathbf{p}_{nui}^t]^t \tag{7}$$

Let $\boldsymbol{\theta}$ denote the vector containing all the true values of the LDP. The location estimation will be based on the estimated value $\widehat{\boldsymbol{\theta}}$ of this vector. The size of $\boldsymbol{\theta}$ is $N_{\boldsymbol{\theta}} = KN_sN_t$, with $K \in \{1, 2, 3, 4\}$ being the number of available different kinds of LDP. For example, for $K = 4$, $\boldsymbol{\theta} = [\mathbf{d}^t, \boldsymbol{\psi}^t, \boldsymbol{\phi}^t, \mathbf{f}_d^t]^t$. Assuming that $\widehat{\boldsymbol{\theta}} \sim N(\boldsymbol{\theta}, \mathbf{C}_{\widetilde{\boldsymbol{\theta}}})$, the FIM, which is a measure of the information about $\mathbf{p}$ contained in $\boldsymbol{\theta}$, is given by

$$\boldsymbol{J} = \frac{\partial \boldsymbol{\theta}^t}{\partial \mathbf{p}} \mathbf{C}_{\widetilde{\boldsymbol{\theta}}}^{-1} \frac{\partial \boldsymbol{\theta}}{\partial \mathbf{p}^t} = \mathbf{G}\mathbf{C}_{\widetilde{\boldsymbol{\theta}}}^{-1}\mathbf{G}^t \tag{8}$$

where we introduced the Jacobian matrix $\mathbf{G} = \frac{\partial \boldsymbol{\theta}^t}{\partial \mathbf{p}}$. To compute the submatrices composing $\mathbf{G}$ lets introduce some key quantities

$$\mathbf{R} \triangleq \mathbf{1}_{N_t}^t \otimes \mathbf{I}_{N_s} \tag{9}$$

$$\mathbf{C}_{\boldsymbol{\phi}} \triangleq diag\{\cos(\phi_{ij})\} \tag{10}$$

$$\mathbf{S}_{\boldsymbol{\phi}} \triangleq diag\{\sin(\phi_{ij})\} \quad . \tag{11}$$

$\mathbf{C}_{\boldsymbol{\psi}}$ and $\mathbf{S}_{\boldsymbol{\psi}}$ are defined similarly. If the MT communicates only with 1 BS through a multipath environment, then $\mathbf{Y}_{bs} = y_{bs}\mathbf{I}$ and $\mathbf{X}_{bs} = x_{bs}\mathbf{I}$. $\mathbf{G}$ is then composed of the following vectors and matrices containing partial derivatives

$$\mathbf{D}_{\mathbf{x}_s} \triangleq \frac{\partial \mathbf{d}^t}{\partial \mathbf{x}_s} = \mathbf{R}(\mathbf{C}_{\boldsymbol{\phi}} + \mathbf{C}_{\boldsymbol{\psi}}) \tag{12}$$

$$\mathbf{D}_{\mathbf{y}_s} \triangleq \frac{\partial \mathbf{d}^t}{\partial \mathbf{y}_s} = \mathbf{R}(\mathbf{S}_{\boldsymbol{\phi}} + \mathbf{S}_{\boldsymbol{\psi}}) \tag{13}$$

$$\mathbf{d}_x^t \triangleq \frac{\partial \mathbf{d}^t}{\partial x_0} = -\mathbf{1}^t\mathbf{C}_{\boldsymbol{\phi}} \;,\; \mathbf{d}_y^t \triangleq \frac{\partial \mathbf{d}^t}{\partial y_0} = -\mathbf{1}^t\mathbf{S}_{\boldsymbol{\phi}} \tag{14}$$

$$\mathbf{d}_{\upsilon_x}^t \triangleq \frac{\partial \mathbf{d}^t}{\partial \upsilon_x} = -(\mathbf{t} \otimes \mathbf{1}_{N_s})^t\mathbf{C}_{\boldsymbol{\phi}} \tag{15}$$

$$\mathbf{d}_{\upsilon_y}^t \triangleq \frac{\partial \mathbf{d}^t}{\partial \upsilon_y} = -(\mathbf{t} \otimes \mathbf{1}_{N_s})^t\mathbf{S}_{\boldsymbol{\phi}} \tag{16}$$

$$\boldsymbol{\Psi}_{\mathbf{x}_s} \triangleq \frac{\partial \boldsymbol{\psi}^t}{\partial \mathbf{x}_s} = -\mathbf{R}(\mathbf{I}_{N_t} \otimes \mathbf{S}_{\boldsymbol{\psi}}\mathbf{D}_{bs}^{-1}) \tag{17}$$

$$\boldsymbol{\Psi}_{\mathbf{y}_s} \triangleq \frac{\partial \boldsymbol{\psi}^t}{\partial \mathbf{y}_s} = \mathbf{R}(\mathbf{I}_{N_t} \otimes \mathbf{C}_{\boldsymbol{\psi}}\mathbf{D}_{bs}^{-1}) \tag{18}$$

$$\boldsymbol{\psi}_x^t \triangleq \frac{\partial \boldsymbol{\psi}^t}{\partial x_0} = \mathbf{0}^t \;,\; \boldsymbol{\psi}_y^t \triangleq \frac{\partial \boldsymbol{\psi}^t}{\partial y_0} = \mathbf{0}^t \tag{19}$$

$$\boldsymbol{\psi}_{\upsilon_x}^t \triangleq \frac{\partial \boldsymbol{\psi}^t}{\partial \upsilon_x} = \mathbf{0}^t \;,\; \boldsymbol{\psi}_{\upsilon_y}^t \triangleq \frac{\partial \boldsymbol{\psi}^t}{\partial \upsilon_y} = \mathbf{0}^t \tag{20}$$

$$\boldsymbol{\Phi}_{\mathbf{x}_s} \triangleq \frac{\partial \boldsymbol{\phi}^t}{\partial \mathbf{x}_s} = -\mathbf{R}\mathbf{S}_{\boldsymbol{\phi}}\mathbf{D}_{mts}^{-1} \tag{21}$$

$$\boldsymbol{\Phi}_{\mathbf{y}_s} \triangleq \frac{\partial \boldsymbol{\phi}^t}{\partial \mathbf{y}_s} = -\mathbf{R}\mathbf{C}_{\boldsymbol{\phi}}\mathbf{D}_{mts}^{-1} \tag{22}$$

$$\boldsymbol{\phi}_x^t \triangleq \frac{\partial \boldsymbol{\phi}^t}{\partial x_0} = \mathbf{1}^t\mathbf{S}_{\boldsymbol{\phi}}\mathbf{D}_{mts}^{-1} \;,\; \boldsymbol{\phi}_y^t \triangleq \frac{\partial \boldsymbol{\phi}^t}{\partial y_0} = -\mathbf{1}^t\mathbf{C}_{\boldsymbol{\phi}}\mathbf{D}_{mts}^{-1} \tag{23}$$

$$\boldsymbol{\phi}_{\upsilon_x}^t \triangleq \frac{\partial \boldsymbol{\phi}^t}{\partial \upsilon_x} = (\mathbf{t} \otimes \mathbf{1}_{N_s})^t\mathbf{S}_{\boldsymbol{\phi}}\mathbf{D}_{mts}^{-1} \tag{24}$$

$$\boldsymbol{\phi}_{\upsilon_y}^t \triangleq \frac{\partial \boldsymbol{\phi}^t}{\partial \upsilon_y} = -(\mathbf{t} \otimes \mathbf{1}_{N_s})^t\mathbf{C}_{\boldsymbol{\phi}}\mathbf{D}_{mts}^{-1} \tag{25}$$

Table 1. Coordinates (m)

$\mathbf{p}_{bs}$	$\mathbf{p}_{mt}$	$\mathbf{x}_s$	$\mathbf{y}_s$
(0,0)	(30,20)	[20,35,25]	[20,15,5]

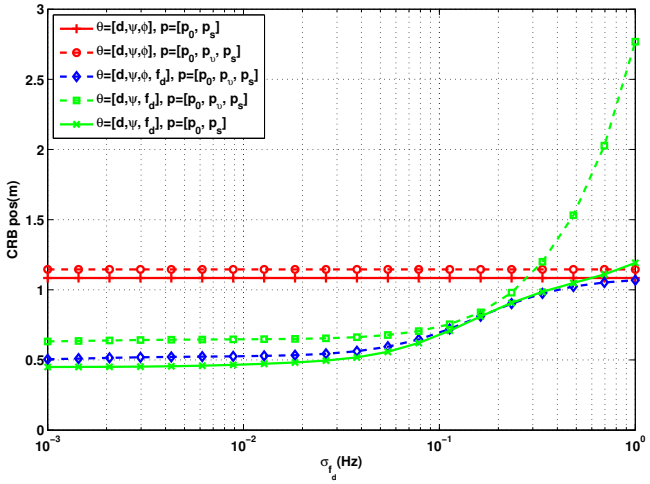

Fig. 2. CRB vs σ_{f_d} at high SNR.

$$\mathbf{F}_{\boldsymbol{\phi}} \triangleq \frac{\partial \mathbf{f}_d^t}{\partial \boldsymbol{\phi}} = -\upsilon_x \mathbf{S}_{\boldsymbol{\phi}} + \upsilon_y \mathbf{C}_{\boldsymbol{\phi}} \tag{26}$$

$$\mathbf{F}_{\mathbf{x}_s} \triangleq \frac{\partial \mathbf{f}_d^t}{\partial \mathbf{x}_s} = \boldsymbol{\Phi}_{\mathbf{x}_s} \mathbf{F}_{\boldsymbol{\phi}} \,,\; \mathbf{F}_{\mathbf{y}_s} \triangleq \frac{\partial \mathbf{f}_d^t}{\partial \mathbf{y}_s} = \boldsymbol{\Phi}_{\mathbf{y}_s} \mathbf{F}_{\boldsymbol{\phi}} \tag{27}$$

$$\mathbf{f}_x^t \triangleq \frac{\partial \mathbf{f}_d^t}{\partial x_0} = \boldsymbol{\phi}_x^t \mathbf{F}_{\boldsymbol{\phi}} \,,\; \mathbf{f}_y^t \triangleq \frac{\partial \mathbf{f}_d^t}{\partial y_0} = \boldsymbol{\phi}_y^t \mathbf{F}_{\boldsymbol{\phi}} \tag{28}$$

$$\mathbf{f}_{\upsilon_x}^t \triangleq \frac{\partial \mathbf{f}_d^t}{\partial \upsilon_x} = \boldsymbol{\phi}_{\upsilon_x}^t \mathbf{F}_{\boldsymbol{\phi}} + \mathbf{1}^t \mathbf{C}_{\boldsymbol{\phi}} \tag{29}$$

$$\mathbf{f}_{\upsilon_y}^t \triangleq \frac{\partial \mathbf{f}_d^t}{\partial \upsilon_y} = \boldsymbol{\phi}_{\upsilon_y}^t \mathbf{F}_{\boldsymbol{\phi}} + \mathbf{1}^t \mathbf{S}_{\boldsymbol{\phi}} \tag{30}$$

4. IDENTIFIABILITY CONDITIONS

According to corollary 1 in [2] (See also [3, Theorem 1]), local identifiability in static environments is feasible if $N_s \geq 2$, while for dynamic environments the condition becomes $(K-1)N_s N_t + N_s \geq 2N_s + 2N_m + 2$. However, in a worst case but also more realistic scenario, the LDP variation can be considered linear for small time intervals [4], so that

$$\boldsymbol{\theta}_k^t = (\mathbf{1} \otimes \boldsymbol{\theta}_{k,0})^t + [\mathbf{0}^t, \ldots, (\mathbf{p}_{N_t-1} - \mathbf{p}_0)^t] \left(\mathbf{I} \otimes \frac{d\boldsymbol{\theta}_{k,0}}{d\mathbf{p}} \right)$$

where the subscript $k \in \{1,2,3\}$ denotes the kind of time-varying LDP, $\boldsymbol{\theta}_{k,0} = \boldsymbol{\theta}_k(\mathbf{p}_0)$ and $\mathbf{p}_0 \triangleq \mathbf{p}$, i.e. the parameters we will estimate, correspond to time instant 0. If a mobility model of order N_m is considered, then $\mathbf{p}_i^t = \mathbf{t}_i^t \mathbf{W}(\mathbf{p}_0)$, where $\mathbf{t}_i^t = [1, \ldots, t_i^{N_m}]$. This allows us to write $\boldsymbol{\theta}_k^t = [\mathbf{t}_0^t \mathbf{V}_k(\mathbf{p}_0), \ldots, \mathbf{t}_{N_t-1}^t \mathbf{V}_k(\mathbf{p}_0)]$ and by taking it's partial derivative with respect to $\mathbf{p}$, we get [5]

$$\frac{\partial \boldsymbol{\theta}_k^t}{\partial \mathbf{p}} = \frac{\partial vec^t\{\mathbf{V}_k^t\}}{\partial \mathbf{p}} (\mathbf{T} \otimes \mathbf{I}_{N_s}) \tag{31}$$

where $\mathbf{T} = [\mathbf{t}_0, \ldots, \mathbf{t}_{N_t-1}]$ is a $(N_m+1) \times N_t$ Vandermonde matrix. From eq. (31) it becomes obvious that the rank of

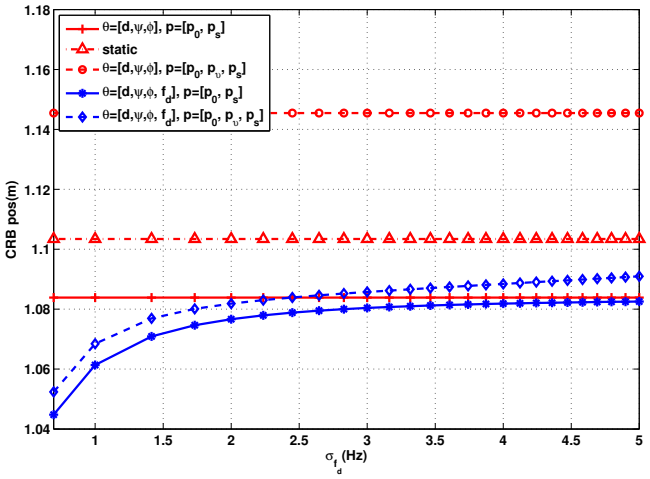

Fig. 3. CRB vs σ_{f_d} at low SNR.

$\mathbf{G} = [\frac{\partial \boldsymbol{\theta}_1^t}{\partial \mathbf{p}}, \ldots, \frac{\partial \boldsymbol{\theta}_K^t}{\partial \mathbf{p}}]$ is limited by the order of the mobility model [6] and thus the condition for identifiability becomes $(K-1)N_s \min\{N_m+1, N_t\} + N_s \geq 2N_s + 2N_m + 2$. Furthermore, for linear movement of the MT, the condition becomes $(2K-3)N_s \geq 4$, which implies that at least $K=3$ different kinds of LDP for at least $N_s = 2$ SB signal components or alternatively $K=4$ different kind of LDP for only $N_s = 1$ SB signal component should be available for localizing the MT. This indicates the significance of the LDP time variation for identifiability purposes.

5. CRAMER-RAO BOUND

The correlation matrix of the parameter estimation errors $\widetilde{\mathbf{p}}$ is bounded below by the inverse of the FIM

$$R_{\widetilde{\mathbf{p}}\widetilde{\mathbf{p}}} = E\{(\widehat{\mathbf{p}} - \mathbf{p})(\widehat{\mathbf{p}} - \mathbf{p})^t\} \geq \mathbf{J}^{-1} \tag{32}$$

Since we are mostly interested in the MT position, we define the lowest achievable position error as the CRB of the position. Based on the FIM, this is given by:

$$CRBpos = \sqrt{tr\{[\mathbf{J}^{-1}]_{(1:2,1:2)}\}} \tag{33}$$

For demonstrating our results we consider a MT that is moving at constant speed $\{\upsilon_x, \upsilon_y\} = \{2, -1.5\} m/sec$ and receives $N_s = 3$ SB components of a signal transmitted by 1 BS. The coordinates of the BS, the MT and the scatterers are given in table 1 and they correspond to a pico-cell. $N_t = 10$ time samples for every LDP estimate are considered and the total observation time is $N_t dt < 1sec$ to ensure that acceleration can be assumed to be negligible.

In this numerical example, we study and compare the CRB for the following scenarios: static ($\mathbf{p}_\upsilon = \mathbf{0}$), dynamic with all LDP available, dynamic with no DS estimates, dynamic with no AoA estimates. For all dynamic scenarios, we examine the case when speed components need to be jointly

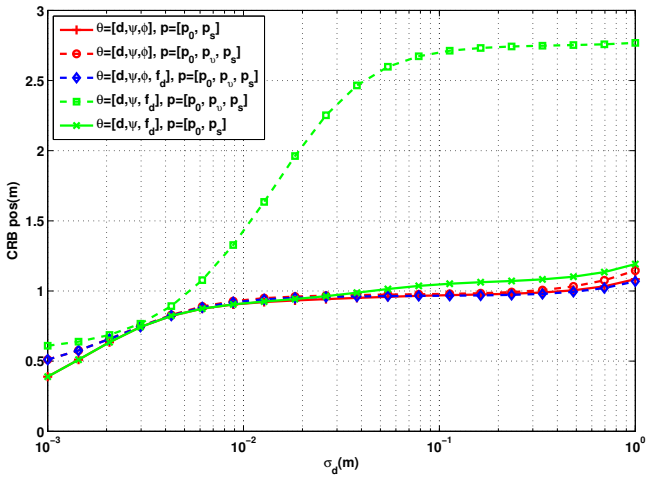

Fig. 4. CRB vs σ_d at high SNR.

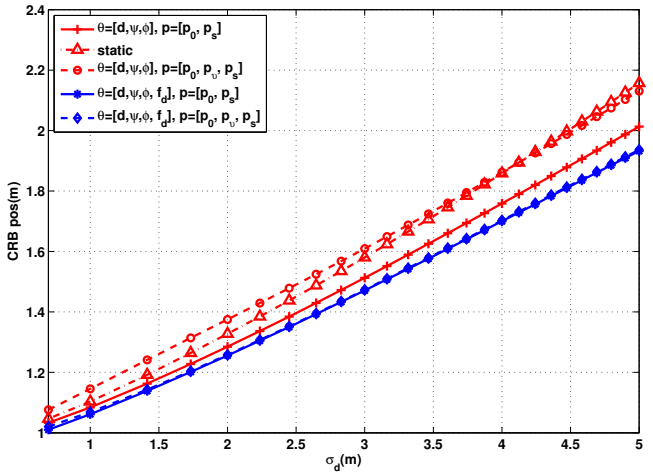

Fig. 5. CRB vs σ_d at low SNR.

estimated ($\mathbf{p}_{int} = [\mathbf{p}_{mt}^t, \mathbf{p}_{\upsilon}^t]^t$) and the case where perfect estimates are available using e.g. inertial sensors ($\mathbf{p}_{int} = \mathbf{p}_{mt}$). We compare the performance for these scenarios either at high SNR $\{\sigma_{f_d} < 1Hz, \sigma_d = 1m\}, \{\sigma_{f_d} = 1Hz, \sigma_d < 1m\}$ or at low SNR $\{\sigma_{f_d} > 1Hz, \sigma_d = 1m\}, \{\sigma_{f_d} = 1Hz, \sigma_d > 1m\}$, while for both cases $\sigma_\phi = \sigma_\psi = 5^o$. The reason for doing so is the low performance of algorithms that do not utilize AoA at low SNR (green curves at fig. 2 and 4), which in turn is a consequence of the fact that in those cases identifiability is possible only due to the LDP time-variation.

From fig. 2 and 4 we observe how sensitive the AoD/delay/DS methods (green curves) are to the accuracy of DS and delays, in contrast to AoD/delay/AoA methods (red curves) that are not so much affected by the accuracy of delays. Actually the performance of these 2 methods can be compared analytically for the case when $\mathbf{p}_{int} = \mathbf{p}_{mt}$. Due to the linear relationship between $\frac{\partial \mathbf{f}_d^t}{\partial \mathbf{p}}$ and $\frac{\partial \phi^t}{\partial \mathbf{p}}$, it can be easily proved that $\mathbf{J}_{noAOA} \geq \mathbf{J}_{noDS}$ when $\sigma_{f_d}^2 / \min_{ij}\{-\upsilon_x sin(\phi_{ij}) + \upsilon_y cos(\phi_{ij})\} \leq \sigma_\phi^2$.

From fig. 3 and 5 we observe that the AoD/delay/AoA method has higher performance in a dynamic scenario with $\mathbf{p}_\upsilon$ known than in a static environment, although one would think that these two are equivalent. We further observe the superiority of the methods that exploit all 4 kinds of LDP, compared to the static case where there is no Doppler. The Doppler estimates seem to enhance performance a lot, especially when $\mathbf{p}_\upsilon$ needs to be estimated. When $\mathbf{p}_\upsilon$ is known, Doppler shifts estimates are useful only if they are more accurate than the AoA estimates, as before.

6. CONCLUSIONS

The purpose of this paper has been two-fold: On one hand the high accuracy of (D)SBM-based localization algorithms in strictly NLoS environment was demonstrated. Sub-meter accuracy for high SNR translated into accurate delay and Doppler shift estimates (no need for very accurate angle estimates) or accuracy close to 1 meter for low SNR can possibly be achieved with efficient estimators. On the other hand we have demonstrated certain advantages that the DSBM-based localization algorithms enjoy over SBM-based ones. These include identifiability in the absence of AoA, even for small LDP time variations and superior performance when all 4 different kinds of LDP are exploited. The results were demonstrated for linear movement of the MT but can be easily generalized to any kind of movement.

7. REFERENCES

[1] H. Miao, K. Yu, and M. J. Juntti, "Positioning for NLOS Propagation: Algorithm Derivations and Cramer-Rao Bounds," *IEEE Trans. Veh. Technol.*, vol. 56, no. 5, pp. 2568 – 2580, 2007.

[2] K. Papakonstantinou and D. Slock, "Identifiability and Performance Concerns in Location Estimation," 2009, Proc. IEEE International Conference on Acoustics, Speech and Signal Processing 2009.

[3] Thomas J. Rothenberg, "Identification in Parametric Models," *Econometrica*, vol. 39, no. 3, pp. 577 – 591, 1971.

[4] K. Papakonstantinou, *Applications of Statistical Signal Processing in Mobile Terminal Localization*, Ph.D. thesis, EURECOM - Telecom Paris, Sophia-Antipolis, France, July 2010.

[5] Jan R. Magnus and Heinz Neudecker, *Matrix Differential Calculus with Applications in Statistics and Econometrics*, John Wiley and Sons, 1999.

[6] G. Marsaglia and G.P.H. Styan, "Equalities and inequalities for ranks of matrices," *Linear and Multilinear Algebra*, vol. 2, pp. 269 – 292, 1974.